STRUCTURAL
CHEMISTRY

Volume 74 (2018)

Supporting information for article:

Synthesis and characterization of self-assembled inorganic–organic hybrid arsenotungstates

Swati Parbhakar, Reetam Kaushik and Firasat Hussain

S1. FT-IR spectra of {[$Cu_2(H_2O)(1,10phen)_2(\mu\text{-}CH_3COO)_2]_4[Ln_2(H_2O)_2(\mu\text{-}CH_3COO)_2(\alpha\text{-}AsW_{11}O_{39})_2]\}^{2-}$ [Ln^{III} = Pr(1a), Nd(2a), Sm(3a), Eu(4a), Gd(5a), Tb(6a), Dy(7a), Ho(8a), Er(9a), Tm(10a), Yb(11a) and Lu(12a)].

S2. UV/Vis spectra of 1a – 12a recorded in aqueous solution in the range of 190-400 nm.

S3. Plots of Kunelka – Munk versus energy E(eV) for 1a – 12a.

S4. Thermogravimetric analysis curves of 1a – 12a.

S5. The change in average bond lengths Ln-O (Å) [Eu^{III} = 2.4194, Gd^{III} = 2.4109, Tb^{III} = 2.3916, Dy^{III} = 2.3838, Ho^{III} = 2.3761, Er^{III} = 2.3595)in the polyanion clusters {[$Cu_2(H_2O)(1,10phen)_2(\mu\text{-}CH_3COO)_2]_4[Ln_2(H_2O)_2(\mu\text{-}CH_3COO)_2(\alpha\text{-}AsW_{11}O_{39})_2]\}^{2-}$ [Ln^{III} = Pr(1a), Nd(2a), Sm(3a), Eu(4a), Gd(5a), Tb(6a), Dy(7a), Ho(8a), Er(9a), Tm(10a), Yb(11a) and Lu(12a)] plotted against the effective ionic radius of lanthanoids.

S6. Comparison of powder XRD and single crystal simulated patterns for compounds 4a – 9a.

S7. Powder XRD plots for the complexes {[$Cu_2(H_2O)(1,10phen)_2(\mu\text{-}CH_3COO)_2]_4[Ln_2(H_2O)_2(\mu\text{-}CH_3COO)_2(\alpha\text{-}AsW_{11}O_{39})_2]\}^{2-}$ [Ln^{III} = Pr(1a), Nd(2a), Sm(3a), Tm(10a), Yb(11a) and Lu(12a)].

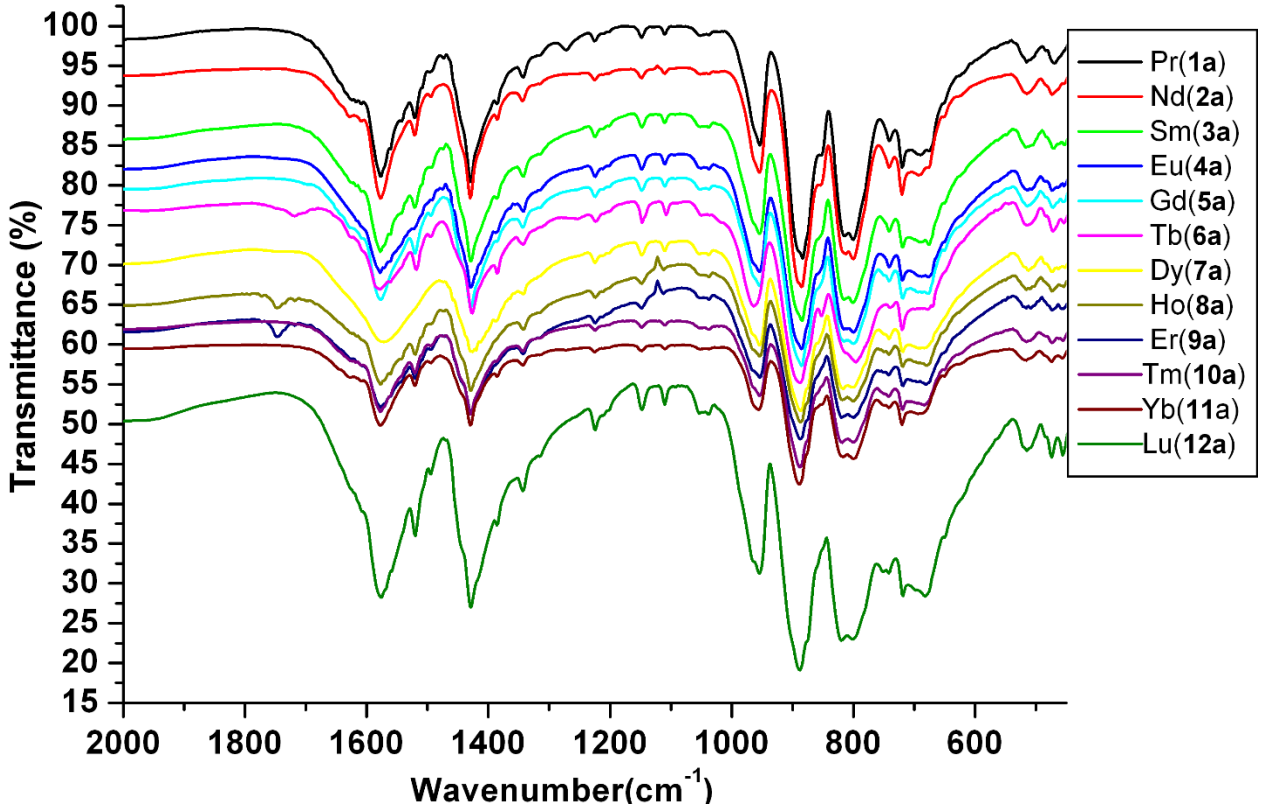

Figure S1 FT-IR spectra of {[$Cu_2(H_2O)(1,10phen)_2(\mu\text{-}CH_3COO)_2]_4[Ln_2(H_2O)_2(\mu\text{-}CH_3COO)_2(\alpha\text{-}AsW_{11}O_{39})_2]\}^{2-}$ [Ln^{III} = Pr(**1a**), Nd(**2a**), Sm(**3a**), Eu(**4a**), Gd(**5a**), Tb(**6a**), Dy(**7a**), Ho(**8a**), Er(**9a**), Tm(**10a**), Yb(**11a**) and Lu(**12a**)].

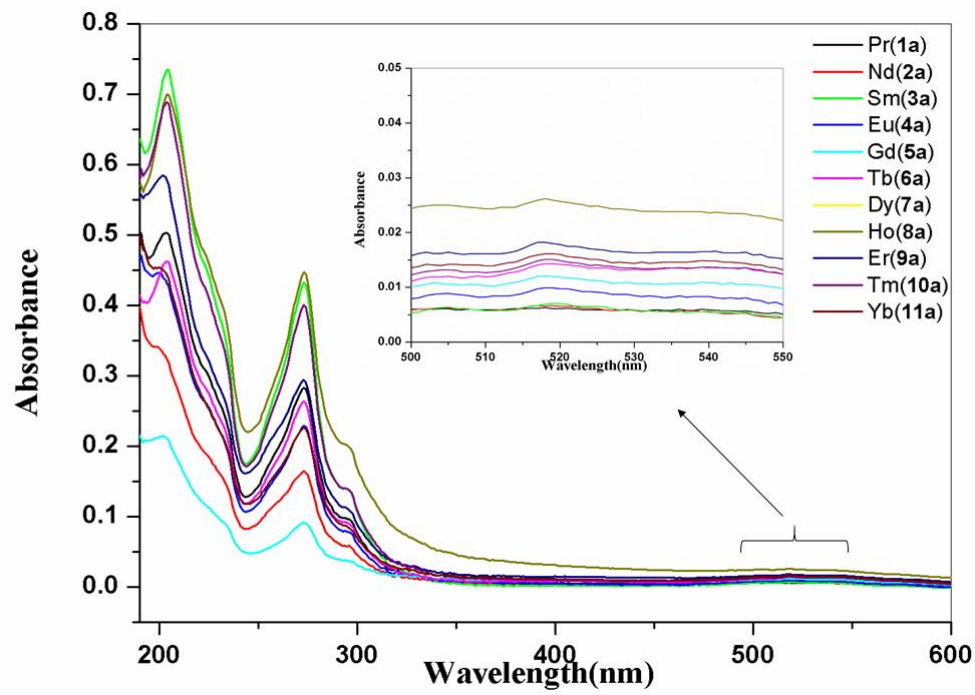

Figure S2 UV-Vis spectra of **1a** – **12a** recorded in aqueous solution in the range of 190-600 nm.

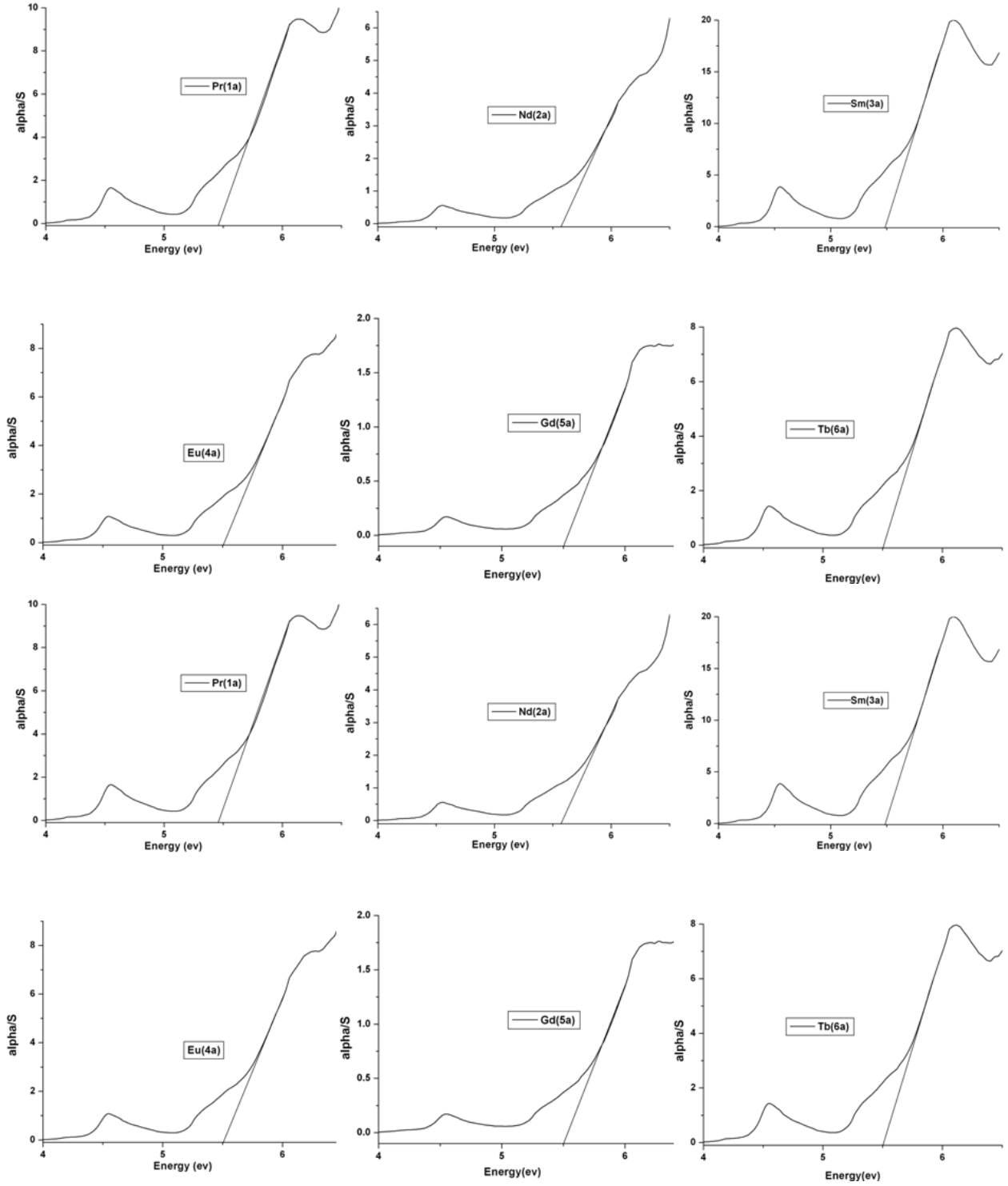

Figure S3 Plots of Kunelka – Munk versus energy E(eV) for **1a** – **12a**.

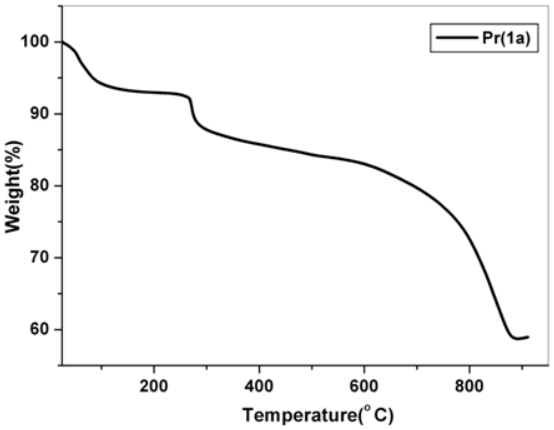
Pr(1a)
Weight(%)
Temperature(°C)

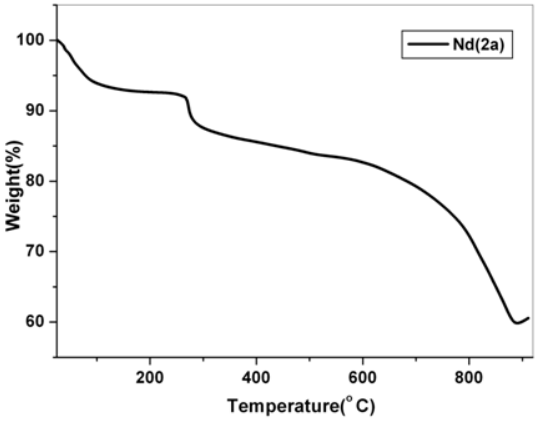
Nd(2a)
Weight(%)
Temperature(°C)

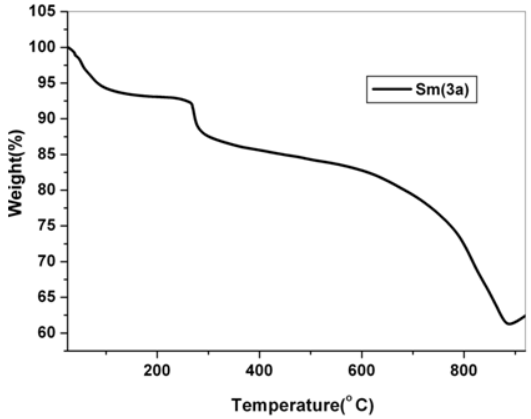
Sm(3a)
Weight(%)
Temperature(°C)

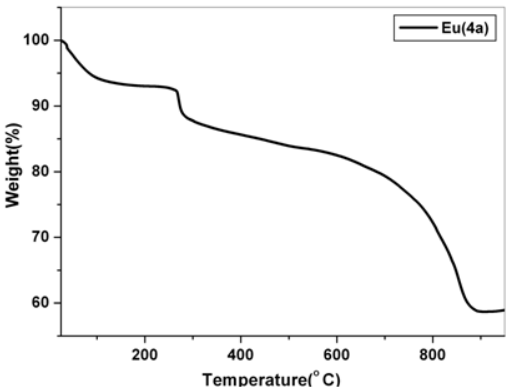
Eu(4a)
Weight(%)
Temperature(°C)

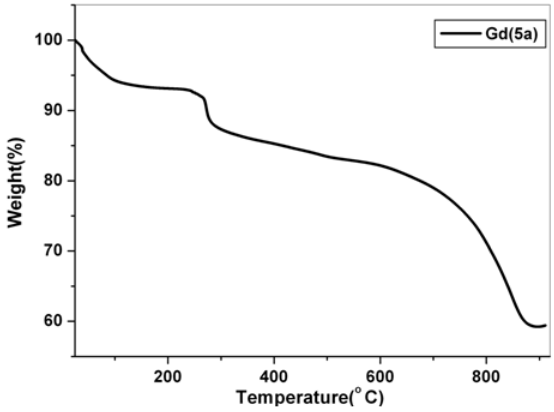
Gd(5a)
Weight(%)
Temperature(°C)

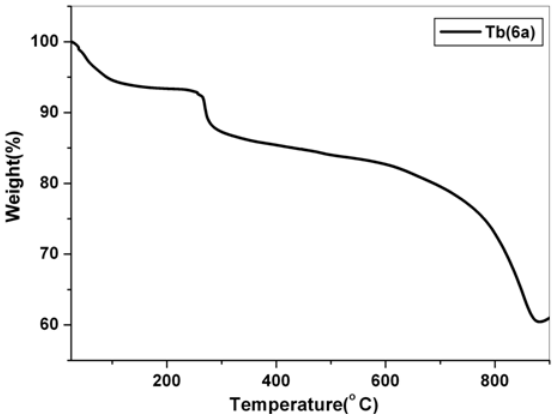
Tb(6a)
Weight(%)
Temperature(°C)

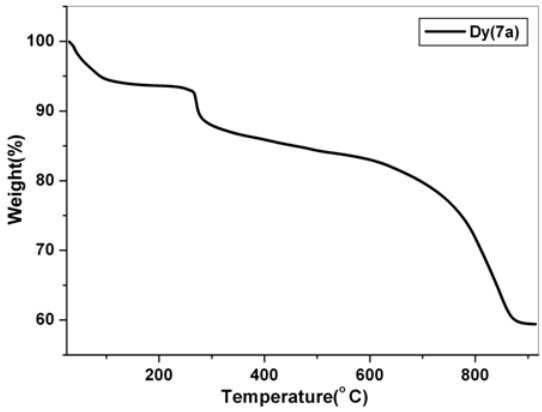
Dy(7a)
Weight(%)
Temperature(°C)

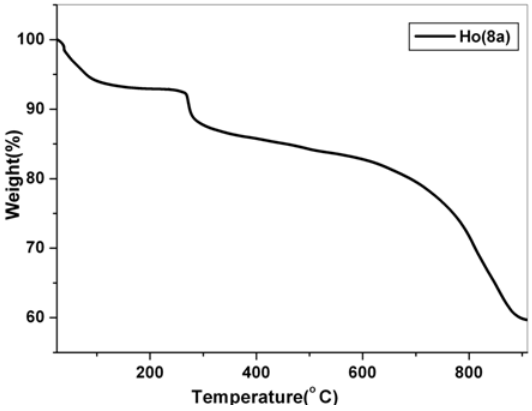
Ho(8a)
Weight(%)
Temperature(°C)

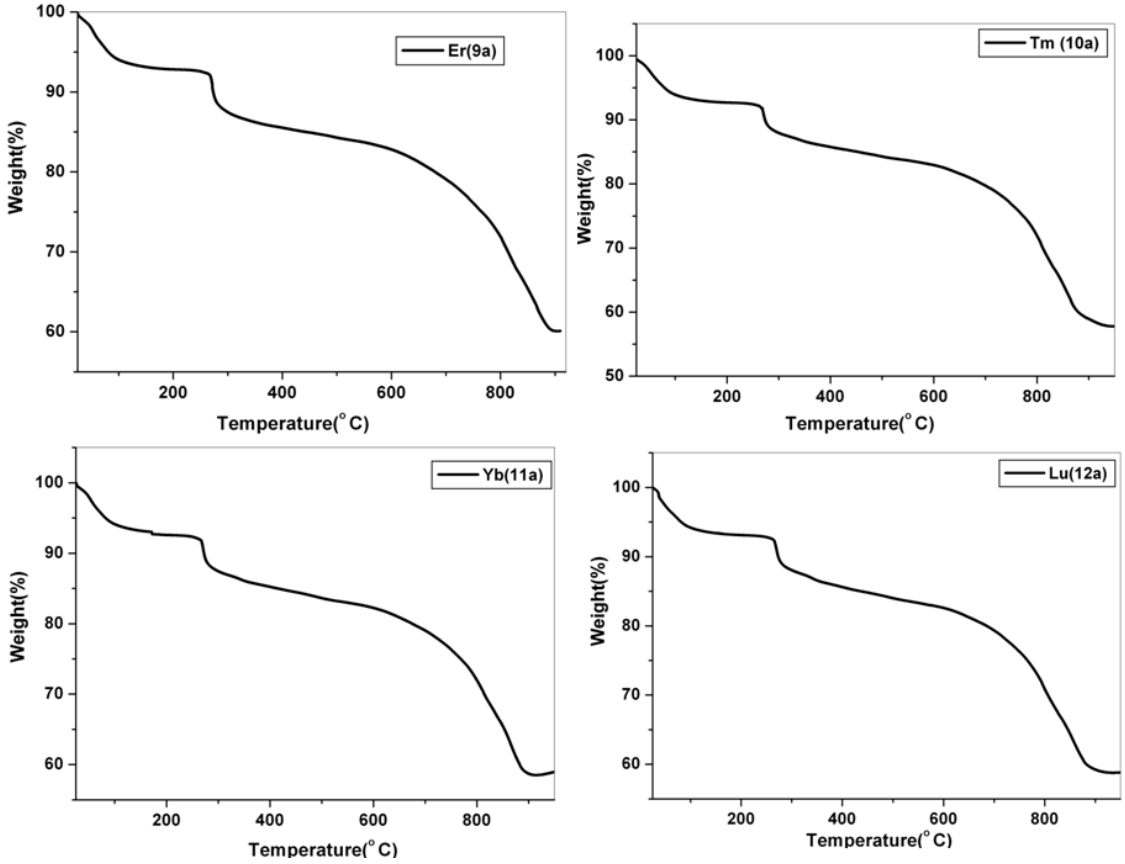

Figure S4 Thermogravimetric analysis curves of **1a** – **12a**.

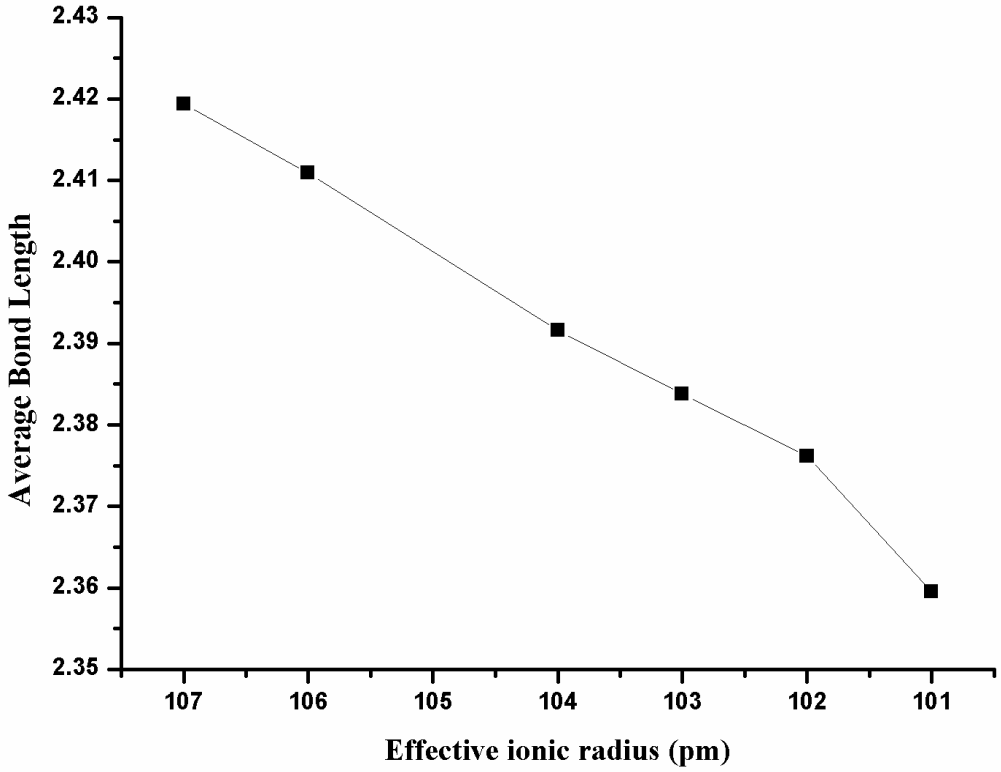

Figure S5 The change in average bond lengths Ln-O (Å) [Eu^{III} = 2.4194, Gd^{III} = 2.4109, Tb^{III} = 2.3916, Dy^{III} = 2.3838, Ho^{III} = 2.3761, Er^{III} = 2.3595)in the polyanion clusters $\{[Cu_2(H_2O)(1,10phen)_2(\mu\text{-}CH_3COO)_2]_4[Ln_2(H_2O)_2(\mu\text{-}CH_3COO)_2(\alpha\text{-}AsW_{11}O_{39})_2]\}^{2-}$ [Ln^{III} = Pr(**1a**), Nd(**2a**), Sm(**3a**), Eu(**4a**), Gd(**5a**), Tb(**6a**), Dy(**7a**), Ho(**8a**), Er(**9a**), Tm(**10a**), Yb(**11a**) and Lu(**12a**)] plotted against the effective ionic radius of lanthanoids.

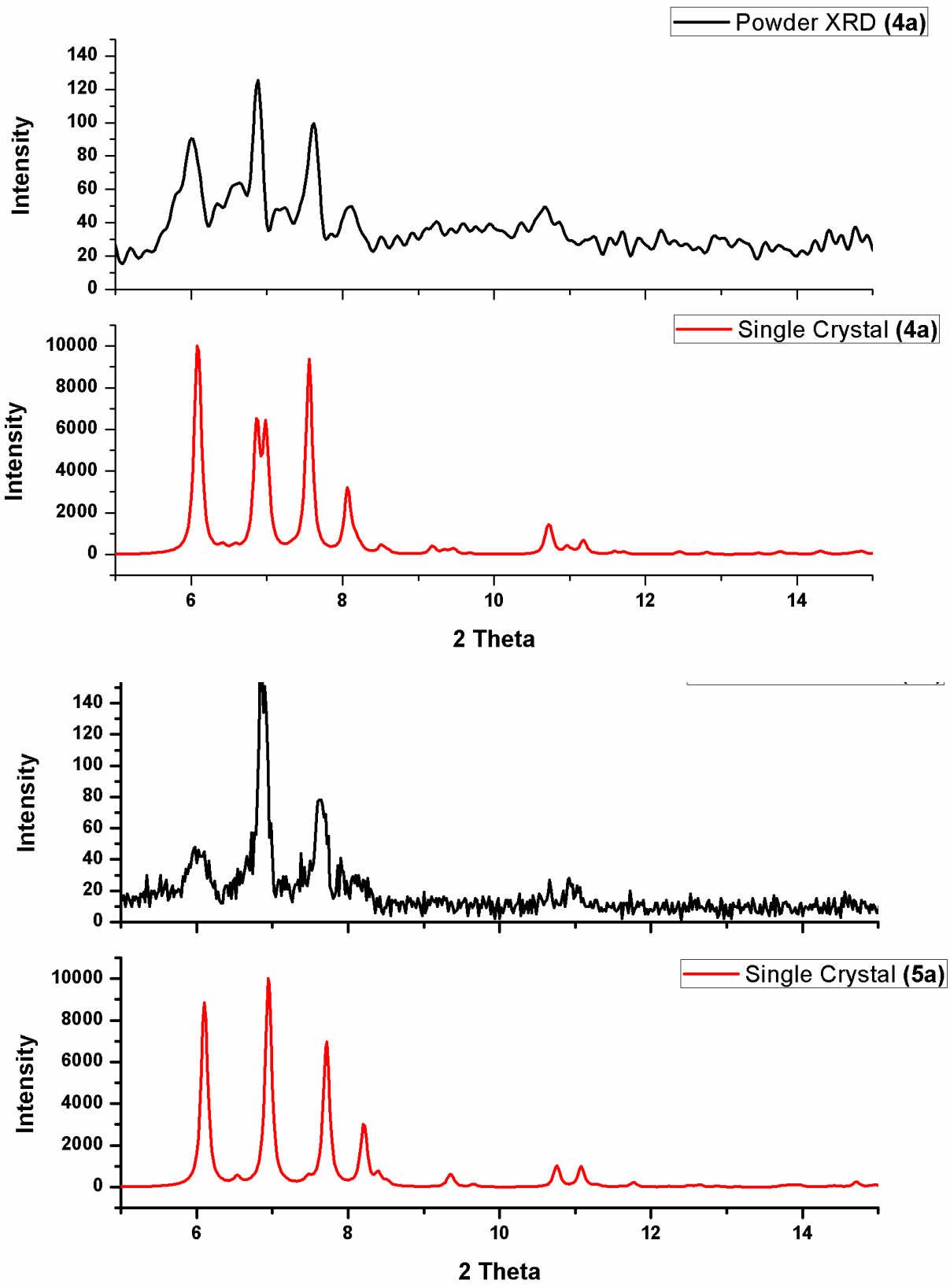
Powder XRD (4a)
Intensity
Single Crystal (4a)
Intensity
2 Theta
Intensity
Single Crystal (5a)
Intensity
2 Theta

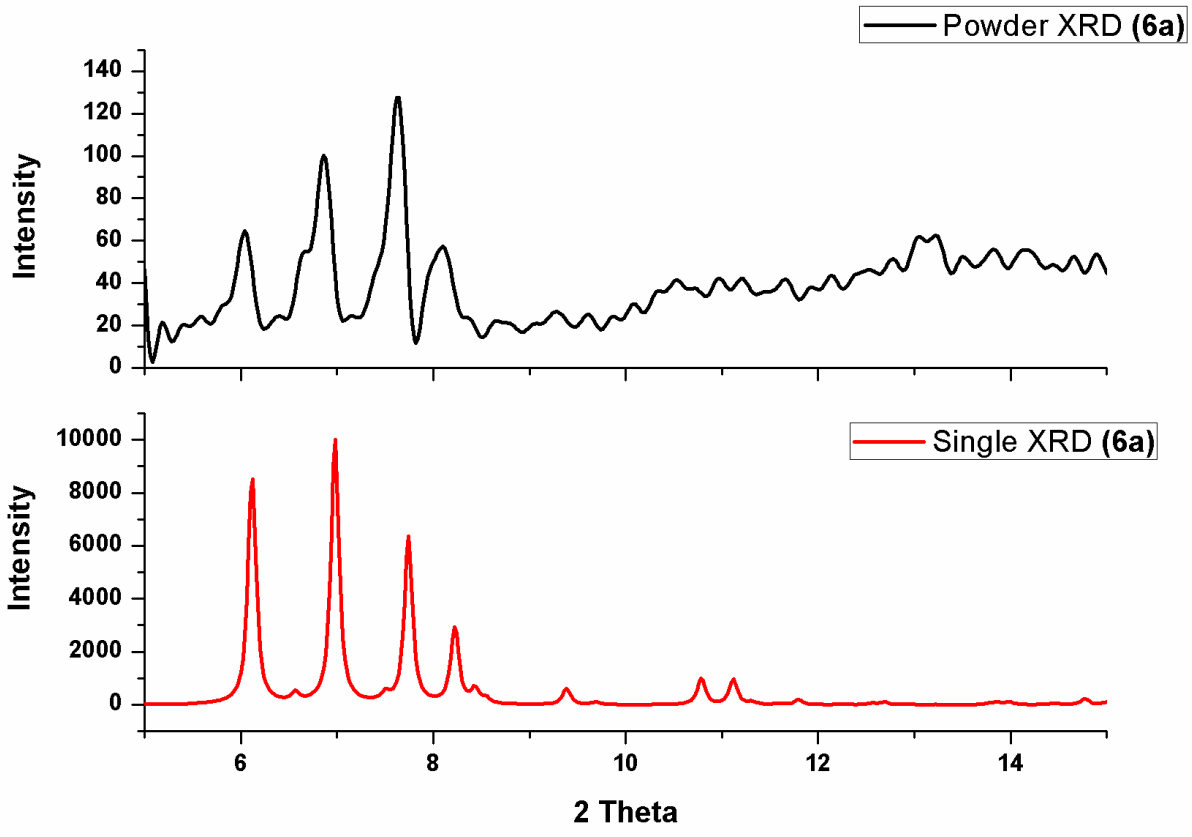
Powder XRD (6a)
Intensity
140
120
100
80
60
40
20
0
Single XRD (6a)
Intensity
10000
8000
6000
4000
2000
0
6
8
10
12
14
2 Theta

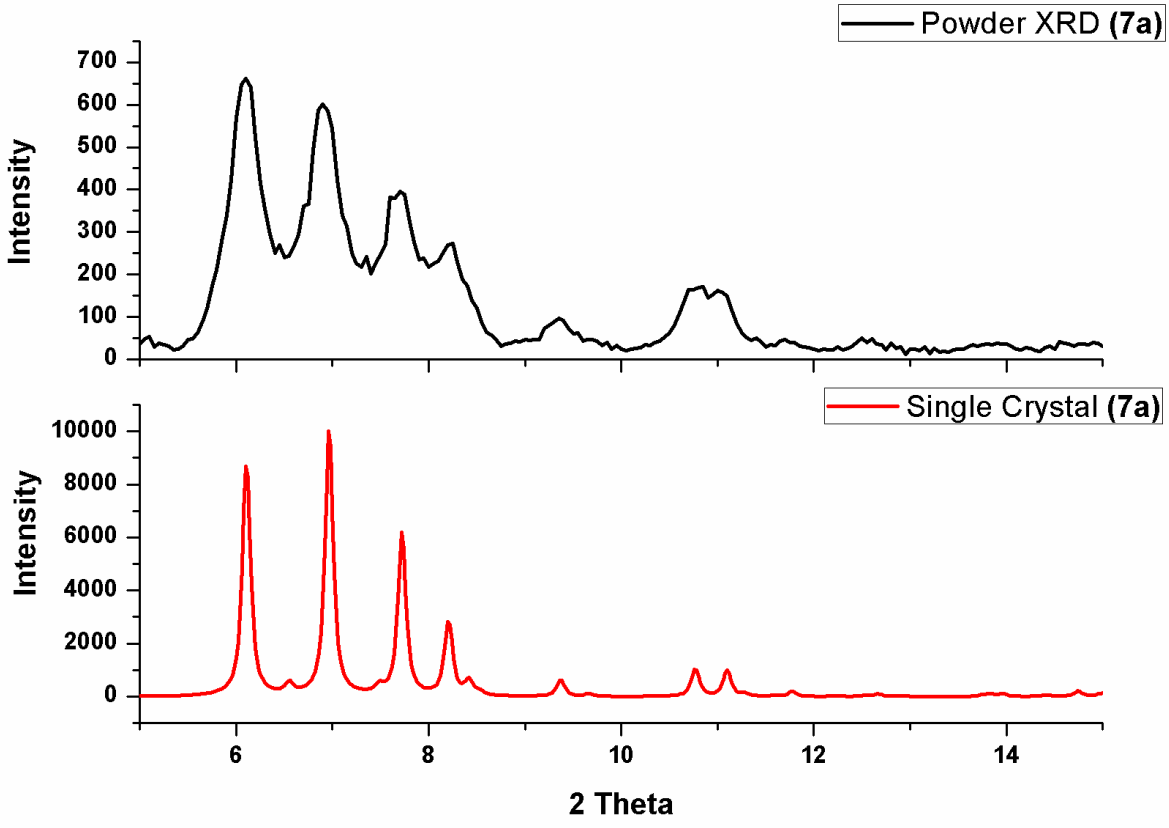
Powder XRD (7a)
Intensity
700
600
500
400
300
200
100
0
Single Crystal (7a)
Intensity
10000
8000
6000
4000
2000
0
6
8
10
12
14
2 Theta

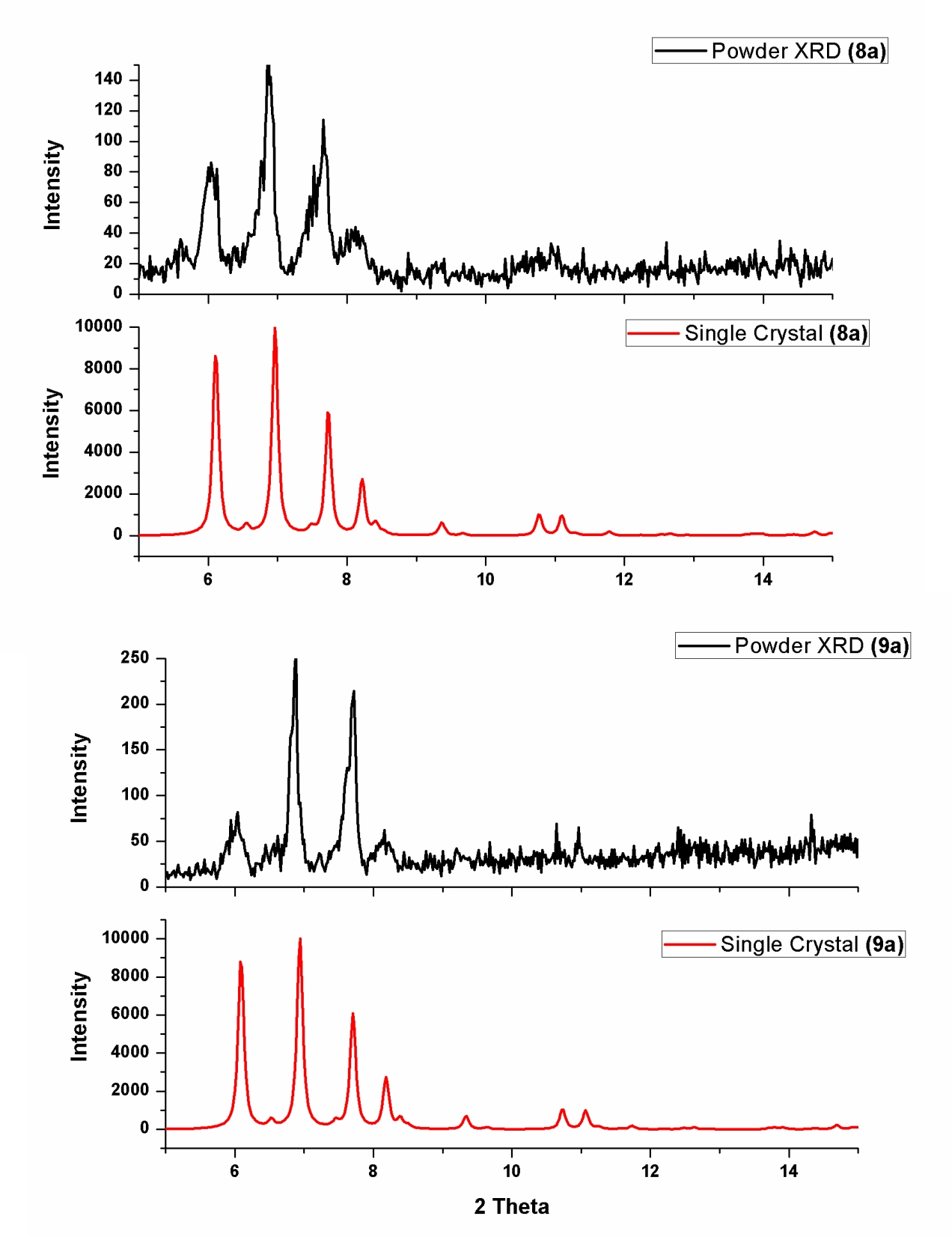

Figure S6 Comparison of powder XRD and single crystal simulated patterns for compounds **4a** – **9a.**

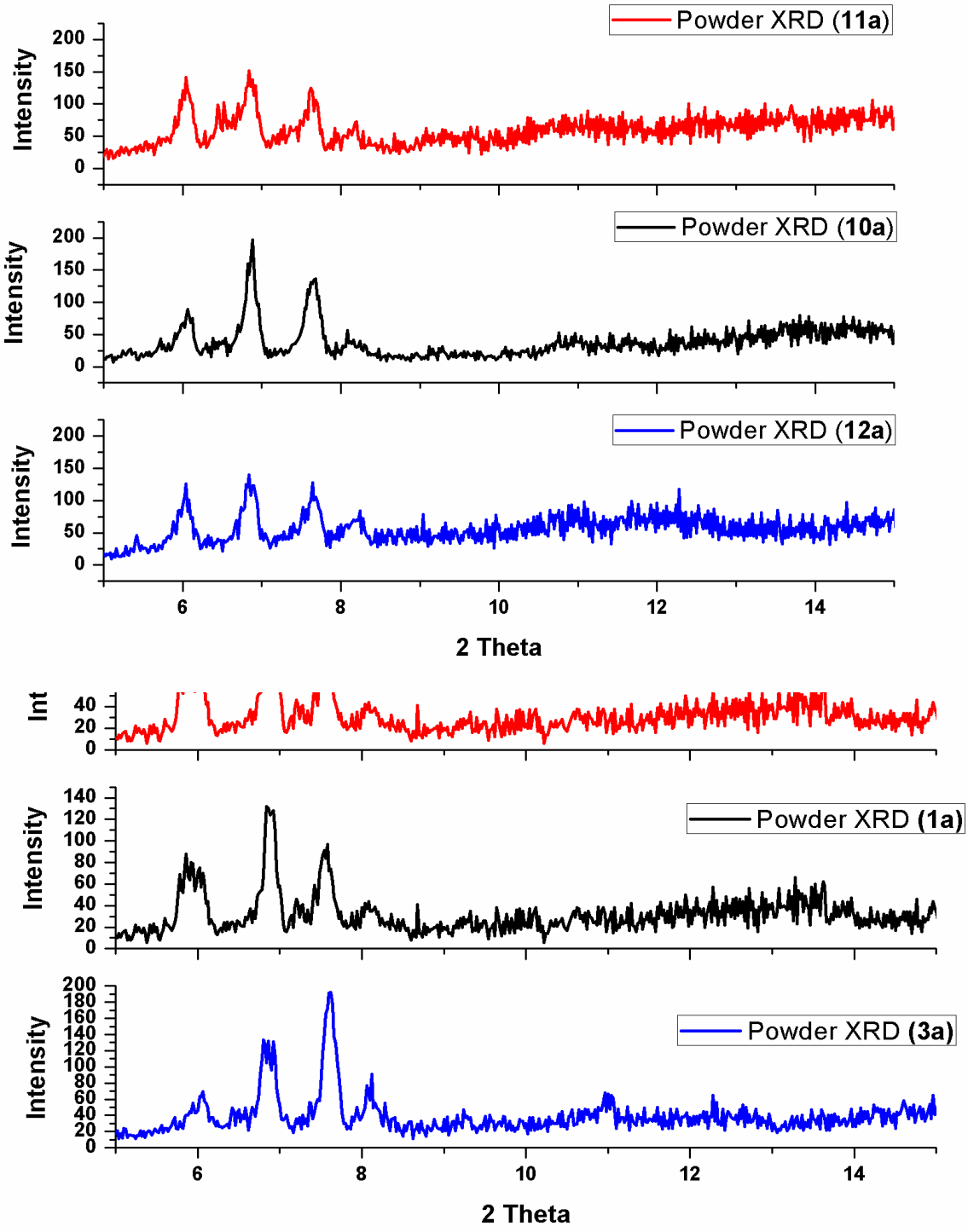

Figure S7. Powder XRD plots for the complexes {[$Cu_2(H_2O)(1,10phen)_2(\mu\text{-}CH_3COO)_2]_4[Ln_2(H_2O)_2(\mu\text{-}CH_3COO)_2(\alpha\text{-}AsW_{11}O_{39})_2]\}^{2-}$ [Ln^{III} = Pr(**1a**), Nd(**2a**), Sm(**3a**), Tm(**10a**), Yb(**11a**) and Lu(**12a**)].